Plant Physiology®

Elicitor-induced plant immunity relies on amino acids accumulation to delay the onset of bacterial virulence

Xiaomu Zhang , Philip J. Tubergen , Israel D.K. Agorsor , Pramod Khadka , Connor Tembe, Cynthia Denbow , Eva Collakova , Guillaume Pilot , and Cristian H. Danna .

- 1 Department of Biology, University of Virginia, Charlottesville, VA 22904, USA
- 2 Department of Molecular Biology & Biotechnology, School of Biological Sciences, College of Agriculture & Natural Sciences, University of Cape Coast, Cape Coast, Ghana
- 3 School of Plant and Environmental Sciences, Virginia Tech, Blacksburg, VA 24060, USA
- *Author for correspondence: cdanna@virginia.edu (C.H.D.)

The author responsible for distribution of materials integral to the findings presented in this article in accordance with the policy described in the Instructions for Authors (https://academic.oup.com/plphys) is Cristian H. Danna.

Abstract

Research Article

Plant immunity relies on the perception of microbe-associated molecular patterns (MAMPs) from invading microbes to induce defense responses that suppress attempted infections. It has been proposed that MAMP-triggered immunity (MTI) suppresses bacterial infections by suppressing the onset of bacterial virulence. However, the mechanisms by which plants exert this action are poorly understood. Here, we showed that MAMP perception in Arabidopsis (*Arabidopsis thaliana*) induces the accumulation of free amino acids in a salicylic acid (SA)-dependent manner. When co-infiltrated with Glutamine and Serine, two of the MAMP-induced highly accumulating amino acids, *Pseudomonas syringae* pv. tomato DC3000 expressed low levels of virulence genes and failed to produce robust infections in otherwise susceptible plants. When applied exogenously, Glutamine and Serine directly suppressed bacterial virulence and growth, bypassing MAMP perception and SA signaling. In addition, an increased level of endogenous Glutamine in the leaf apoplast of a gain-of-function mutant of *Glutamine Dumper-1* rescued the partially compromised bacterial virulence- and growth-suppressing phenotype of the SA-induced deficient-2 (sid2) mutant. Our data suggest that MTI suppresses bacterial infections by delaying the onset of virulence with an excess of amino acids at the early stages of infection.

Introduction

Plants are remarkably resistant to microbial infections. Only specialized microbes with evolved mechanisms to suppress inducible plant defense responses can cause disease (Abramovitch and Martin 2004). Leaf bacterial pathogens initiate infections by breaching the stomatal barrier at the leaf surface and gaining access to the leaf apoplast, the water- and nutrient-rich intercellular space in the leaf mesophyll (Xin and He 2013). In the leaf apoplast, invading bacteria spend the first 5 h without growing and adapting their metabolism to the new and rapidly changing apoplastic environment (Xin and He 2013). Early in the interaction, both plant and bacterial cells perceive each other and activate transcriptional and metabolic programs tailored to gain control over each

other (Preston 2017). While plant responses evolved to suppress infection attempts, bacterial responses evolved to allow rapid adjustment to the leaf apoplastic environment, suppress plant defense responses, and promote leaf colonization (Yu et al. 2013; O'Leary et al. 2016). Plants recognize invading bacteria by their unique suite of molecules or activity patterns, generally known as microbe-associated molecular pat-(MAMPs). Plant-encoded pattern-recognition receptors perceive MAMPs at the cell surface and activate defense responses collectively known as MAMP-triggered immunity (MTI; also known as pattern-triggered immunity or PTI) (Gómez-Gómez et al. 1999; Nicaise et al. 2009). At the cellular level, MTI early responses include the activation of mitogen-activated protein-kinases, cytoplasmic Ca2+ influx,

membrane depolarization, extracellular medium alkalinization, production of reactive oxygen species, and genomewide transcriptional reprogramming (Granado et al. 1995; Jeworutzki et al. 2010; Maintz et al. 2014; Bigeard et al. 2015). Late MTI responses include the synthesis and accumulation of defense signaling molecules salicylic acid (SA) and ethylene (Gómez-Gómez et al. 1999; Asai et al. 2002; Lecourieux et al. 2005), the synthesis and accumulation of amino acid-derived secondary metabolites, the closing of the stomata, and the reinforcement of plant cell walls via callose and lignin deposition (Adams-Phillips et al. 2009; Clay et al. 2009; Chezem et al. 2017). Ultimately, MTI responses suppress bacterial growth via several mechanisms that act synergistically and coordinately. Suppressing MTI is a critical step in colonizing the plant host (Abramovitch and Martin 2004). Nonpathogenic bacteria fail to suppress MTI responses, cannot adjust their metabolism to the rapidly changing leaf apoplast environment, and succumb within the first hours of the attempted colonization (Hauck et al. 2003; Clay et al. 2009). Bacterial pathogens, however, have evolved virulence mechanisms to suppress MTI early in the interaction (Xin et al. 2018). After entering the leaf apoplast, Pseudomonas syringae pv. tomato DC3000 (PstDC3000) perceives Arabidopsis (Arabidopsis thaliana) metabolites and induces the synthesis of Type-3 secretion system (T3SS) secretory proteins, secreted T3SS effector proteins (T3E), and the SA-antagonist molecule coronatine (COR), all of which have a concerted activity suppressing plant defense (Bender et al. 1987; Brooks et al. 2005; Zhang et al. 2008; Xin and He 2013).

Recent studies have shown that Arabidopsis plants that had been exposed to MAMPs and allowed to proceed with the MTI program for 24 h suppressed the induction of PstDC3000 T3SS, T3E, and COR biosynthesis genes (Lovelace et al. 2018; Nobori et al. 2018; Smith et al. 2018), suggesting that MTI suppresses bacterial growth via suppressing virulence. The MTI-mediated suppression of bacterial virulence seems to rely on changes in the metabolite composition of the leaf apoplast. Arabidopsis seedlings exposed to elf26, a 26 amino acid-long synthetic peptide containing the minimal epitope of bacterial translation Elongation Factor-Tu, suppressed the onset of PstDC3000 virulence via lowering the availability of citric acid, aspartic acid, and 4-benzoic acid (Anderson et al. 2014). Similarly, the perception of flg22, a 22 amino acid-long synthetic peptide containing the minimal epitope of bacterial flagellin, induced changes in sugar concentrations in the leaf apoplast of Arabidopsis that compromised the onset of PstDC3000 virulence (Yamada et al. 2016). Overall, these studies suggest that MAMP perception elicits changes in the concentration of plant metabolites in the leaf apoplast that affect bacterial virulence and growth.

In addition to sugar polymers, secreted proteins, and complex secondary metabolites, primary plant metabolites such as hexoses and free L-amino acid (hereinafter referred to as

"L-AA"), are among the most abundant metabolites in the Arabidopsis leaf apoplast. Notably, some of these metabolites (e.g. glucose and several L-AA) suffice to support PstDC3000 growth and regulate the expression of PstDC3000 virulence genes in vitro, suggesting a critical function for these metabolites in controlling bacterial infections (Rahme et al. 1992; Rico and Preston 2008; Park et al. 2010; Anderson et al. 2014; Chatnaparat et al. 2015a, 2015b; Yamada et al. 2016). In addition, organic acids, gamma-aminobutyric acid (GABA), and some L-AA accumulate at lower millimolar concentrations in Cladosporium fulvum-infected tomato leaf (Solomon and Oliver 2001, 2002). Similarly, GABA and several proteogenic L-AA accumulate to high concentrations in the leaf of P. syringae-infected Arabidopsis and bean (Phaseolus vulgaris) plants (Ward et al. 2010; O'Leary et al. 2016), suggesting that these metabolites could play a role in defense or susceptibility to pathogens.

In a previous study, we presented evidence that flg22 perception elicits changes in both, L-AA transport activity and extracellular L-AA concentrations. Importantly, high concentrations of extracellular L-AA promoted bacterial growth in mock-treated seedlings but suppressed bacterial growth when MTI was elicited 24 h prior to the inoculation (Zhang et al. 2022). The present study aimed at addressing the mechanisms by which flg22-elicited changes in L-AA concentrations impact the growth of PstDC3000. Here, we present evidence that Gln and Ser, among other less represented L-AAs, accumulate in flg22-treated leaves and leaf apoplast of Arabidopsis plants. The MTI-induced increased concentration of L-AA depends on an intact SA-mediated signaling pathway and suffices to suppress PstDC3000 virulence and growth, suggesting MAMP-elicited accumulation of L-AA plays a pivotal role in suppressing bacterial infections. Overall, our data provide insights into how MAMP perception leads to metabolite changes that confer enhanced immunity to bacterial infections.

Results

MAMP perception elicits the accumulation of amino acids in flg22-treated leaves

Amino acids transport activity and the extracellular concentrations of L-AA dynamically change in response to MAMPs perception in liquid-grown 10-d-old Arabidopsis seedlings (hereafter referred to as "seedlings"). Extracellular L-AA concentrations increase within 2 to 4 h posttreatment (HPT) and drop between 8 and 24 HPT with MAMPs (Zhang et al. 2022). In agreement with our previously published data, the flg22-induced enhanced L-AA uptake activity led to a significant increase in L-AA concentration in flg22-treated compared to mock-treated seedlings (Fig. 1A). To determine if, like in seedlings, the elicitation of MTI leads to changes in L-AA concentrations in treated

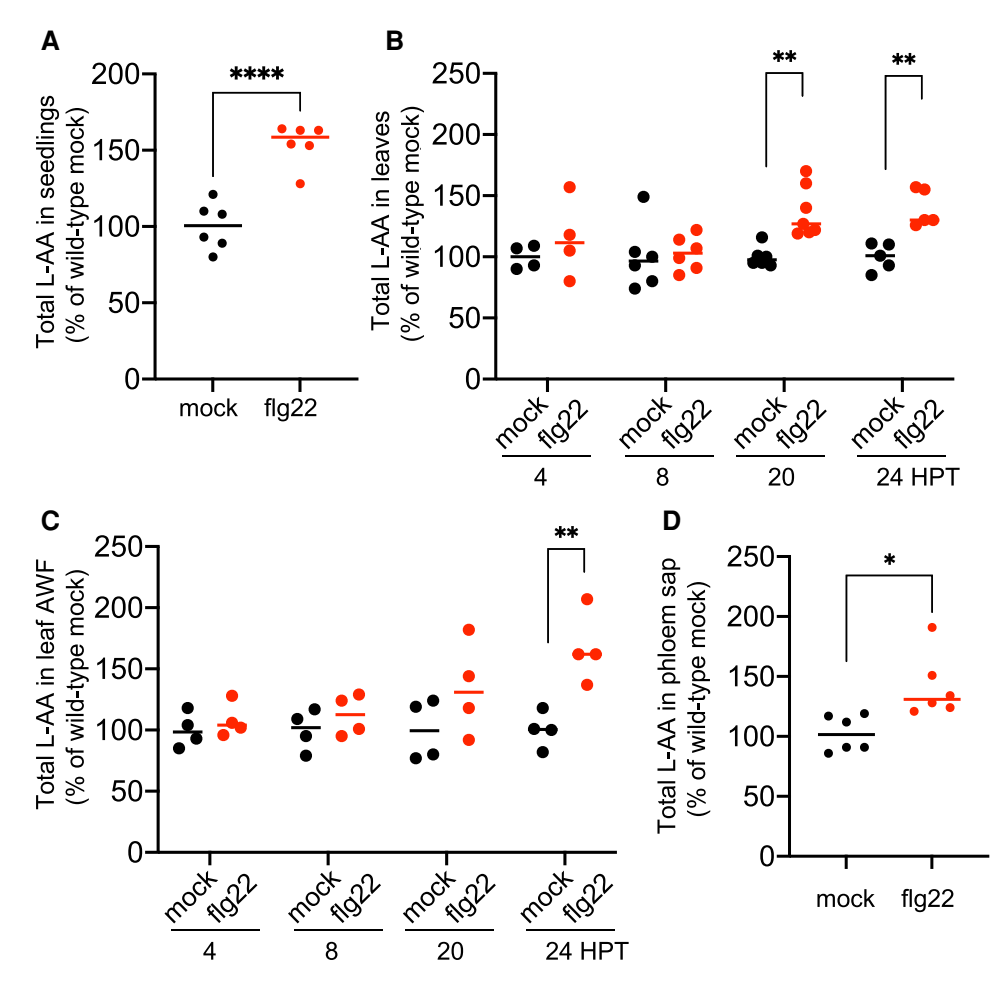


Figure 1. The perception of flg22 induces the accumulation of amino acids in treated leaves. A) Concentrations of L-AA in eleven-day-old seedlings 24 h post-treatment (HPT) with water (mock) or flg22. B) Total L-AA in leaves of wild-type plants after infiltration of leaves with water (mock) or flg22. C) Total L-AA in leaf apoplastic washing fluids of wild-type plants treated with water (mock) or flg22, 24 HPT. D) Total L-AA in the phloem sap of wild-type leaves 24 HPT. Statistical analysis: Welch t-test (A) and t-tests for (B-D) at P values ≤ 0.05 (*), ≤ 0.01 (**), and ≤ 0.0001 (****). All figures show one representative experiment from at least 3 independent experiments.

leaves and leaf apoplast of 6-wk-old plants (hereafter referred to as "plants"), the concentration of L-AA was assessed in fully expanded mature leaves at 4, 8, 20, and 24 HPT with flg22. Like in whole seedlings, L-AA concentrations in leaves increased by 20 HPT (Fig. 1B) and in the leaf apoplastic wash fluids (AWFs) by 24 HPT with flg22 (Fig. 1C). The flg22-receptor mutant fls2 did not accumulate L-AA in leaf tissue in response to the flg22 treatment (Supplemental Fig. S1), demonstrating that L-AA accumulation in treated leaves is a signaling-dependent process initiated by the FLS2 receptor. To define which L-AA contribute to increasing the concentrations of total L-AA following flg22 perception, leaves were water-infiltrated (mock-treated) or infiltrated with flg22 and then collected for L-AA extraction and profiling 24 HPT. Except for Thr and Pro, which remained unchanged, all L-AA detected in leaf samples seemed to accumulate in response to flg22 perception, with Ala, Asn, Gln, Glu, Gly, His, Phe, Ser, and Val increasing significantly compared to mock-treated samples (Table 1). The increased concentration of L-AA elicited by flg22 also led to an increase in L-AA concentrations in the phloem sap 24 HPT (Fig. 1D), suggesting a net mobilization of L-AA out of the treated leaves.

Amino acids that accumulate in MTI-elicited leaves directly suppress bacterial virulence and growth

Free L-AAs are the major form of organic nitrogen in the leaf apoplast. Independent studies have reported concentrations of 2 to 4 mM total L-AA in the leaf apoplast of Arabidopsis (Pilot et al. 2004; Hirner et al. 2006; Yang et al. 2014) tomato (Rico and Preston 2008), and beans (Lohaus et al. 2001; O'Leary et al. 2016), showing that the leaf apoplast is a nitrogen-rich environment. Similar concentrations were detected in our study, with Gln, Ser, Glu, Asp, and Ala representing approximately 80% of all L-AA detected in the leaf AWF of naïve wild-type plants. These AAs accumulated significantly in response to flg22 perception in wild-type plants

Table 1. Concentrations of individual amino acids in leaf apoplastic washing fluids of wild-type and *sid*2 plants 24 h posttreatment with water (mock) or 1 μM flg22

	mock Mean	SEM	flg22 Mean	SEM	Adjusted P-value	
Ala	142.9	7.3	216.3	5	2.44×10^{-8}	a
Arg	6.8	0.4	7.3	0.4	8.49×10^{-1}	
Asn	47	2.7	58.3	2.7	4.75×10^{-2}	a
Asp	285	8.9	291.5	8.5	9.38×10^{-1}	
Gln	277.9	16.8	352.7	19.1	4.75×10^{-2}	a
Glu	342.3	14.2	527.9	15.8	6.10×10^{-9}	a
Gly	38.2	2.8	96.8	8.3	1.07×10^{-6}	a
His	4.7	0.2	8	0.6	9.48×10^{-5}	a
lle	3.9	0.2	6.3	1	1.70×10^{-1}	
Leu	5.9	0.6	9.9	1.8	1.97×10^{-1}	
Lys	6.8	0.6	8.8	0.9	3.12×10^{-1}	
Phe	5.5	0.3	12.7	1.1	3.44×10^{-6}	a
Pro	29.6	3.9	28.2	4.9	9.38×10^{-1}	
Ser	158	7.6	226.3	8.2	8.50×10^{-6}	a
Thr	86.5	3.4	84.7	2.7	9.38×10^{-1}	
Val	11.8	0.4	18.6	1.8	5.46×10^{-3}	a
Total	1452.8		1954.3			

aStatistically significant differences at $P \le 0.05$ between wild-type mock- and flg22-treated leaves. Concentrations of free L-AA (pmol/mg DW) in extracts of water-(mock) or flg22-treated wild-type leaves 24 h posttreatment. Mean \pm SEM of mock (n=18) and flg22 (n=17) samples from 4 independent experiments. Data were analyzed with multiple Welch t-test; P-values were adjusted by 2-stage step-up false discovery rate method (Q=0.01).

(Supplemental Table S1). Several L-AAs that accumulated in the leaf apoplast have been shown to modulate bacterial growth and virulence gene expression in vitro (Rahme et al. 1992; Rico and Preston 2008; Chatnaparat et al. 2015b), suggesting that changes in amino acid concentrations in planta could modulate bacterial infections. To elucidate the potential biological function of increased L-AA concentrations in plant immunity, we sought to bypass MAMP perception with the exogenous supplementation of individual L-AA and assess their impact on PstDC3000 growth in the leaf apoplast. To this end, 2 pilot tests were performed to set the conditions for future experiments. A pilot experiment using radiolabeled Pro, Gln, and Ser showed that these L-AAs were quickly removed from the apoplast by plant cells upon infiltration (Supplemental Fig. S2). These data indicated that amino acids must be co-infiltrated with bacteria to ensure that PstDC3000 is exposed to the high L-AA concentrations found in the leaf apoplast of MTI-elicited plants. Having set up the timing for L-AA supplementation, a second pilot experiment determined the amino acid concentrations to be used. As Gln and Ser are the 2 most highly represented L-AA that accumulate in the leaf apoplast of flg22-treated plants, we initially tested the effect of these 2 L-AA on PstDC3000 growth in plants that were never treated to elicit MTI (hereafter referred to as naïve plants). The data showed that the co-infiltration of PstDC3000 with 10 mM Gln + Ser reproducibly inhibited bacterial growth 48 h postinoculation compared to nonsupplemented PstDC3000 (Supplemental Fig. S3), while the results were inconclusive with 1 mM concentration. To control for the potential toxic effect of high Gln and Ser levels on bacterial growth, PstDC3000 was grown in M9 minimal medium supplemented with increasing concentrations of these L-AA. The data show that both Gln and Ser, alone or combined, not only were not toxic but also significantly promoted bacterial growth at concentrations of 1 and 10 mM, while 0.1 mM did not affect bacterial growth (Supplemental Fig. S4). In addition, to control for the potential context-specific toxicity of amino acid supplementation in the leaf apoplastic environment, bacterial survival was assessed at 3 HPI in naïve plants. The data showed that Gln and Ser supplementation did not affect bacterial numbers at the early stages of infection (Supplemental Fig. S5). These data ruled out the possibility that the lower bacterial counts observed at 48 HPI in Gln- and Ser-supplemented bacteria could originate from a smaller bacterial inoculum in the supplemented plants compared to nonsupplemented controls. Having confirmed the lack of toxicity at the used concentrations, bacteria were supplemented with 10 mM of every individual L-AA that accumulates in flg22-treated leaves to test their impact on bacterial leaf colonization. While most L-AA did not affect PstDC3000 growth, His had a growth-promoting effect, and Gln, Ser, and Val suppressed bacterial growth (Fig. 2A).

Previous studies have shown that an exogenous supply of 20 mM Glu induced SA signaling-mediated defense responses in Arabidopsis plants 5 d after treatment (Goto et al. 2020). Similarly, 100 mM Glu supplementation rapidly elicited Arabidopsis local defense responses that propagated systemically via rapid changes in cytoplasmic calcium fluxes (Toyota et al. 2018). Notwithstanding the use of lower concentrations of amino acids in our experiments, the evidence reported by Goto et al. (2020) and Toyota et al. (2018) warranted testing the potential for Gln and Ser to induce defense responses in our experiments. If 10 mM Gln + Ser supplementation had a plant defense-inducing activity, these amino acids could indirectly suppress bacterial growth by eliciting plant defense. To test this possibility, we assessed the expression of MTI and SA defense-related marker genes in naïve plants supplemented with Gln and Ser. We infiltrated leaves of naïve plants with Gln + Ser alone or coinfiltrated PstDC3000 with Gln + Ser and assessed plant defense responses by monitoring the expression of the early induced defense marker genes CYP81F2 (Cytochrome P450 monooxygenase 81F2) and WRKY29 (transcription factor WRKY29), and the late-induced defense genes ICS1 (isochorismate synthase-1) and PR1 (pathogenesis related-1). While WRKY29 encodes a transcription factor that positively regulates flg22-elicited immunity, CYP81F2 codes for an enzyme needed for synthesizing indole glucosinolates and callose deposition in response to flg22 perception (Clay et al. 2009). Infiltration of leaves with Gln + Ser alone did not induce genes CYP81F2 MTI marker and WRKY29 (Supplemental Fig. S6A). However, the SA biosynthesis gene ICS1 and the SA defense marker gene PR1 were modestly but significantly induced 24 h after Gln + Ser infiltration (Supplemental Fig. S6B). These data suggest that Gln and/

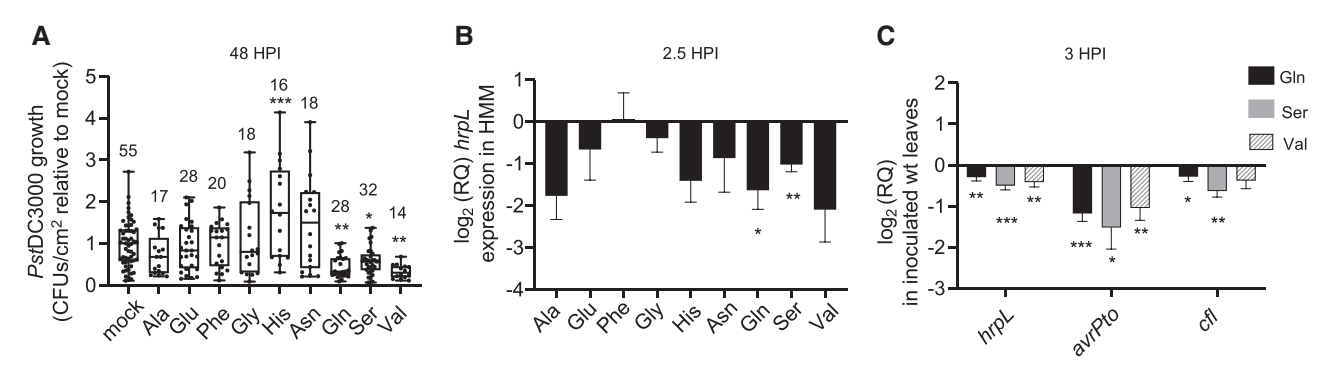


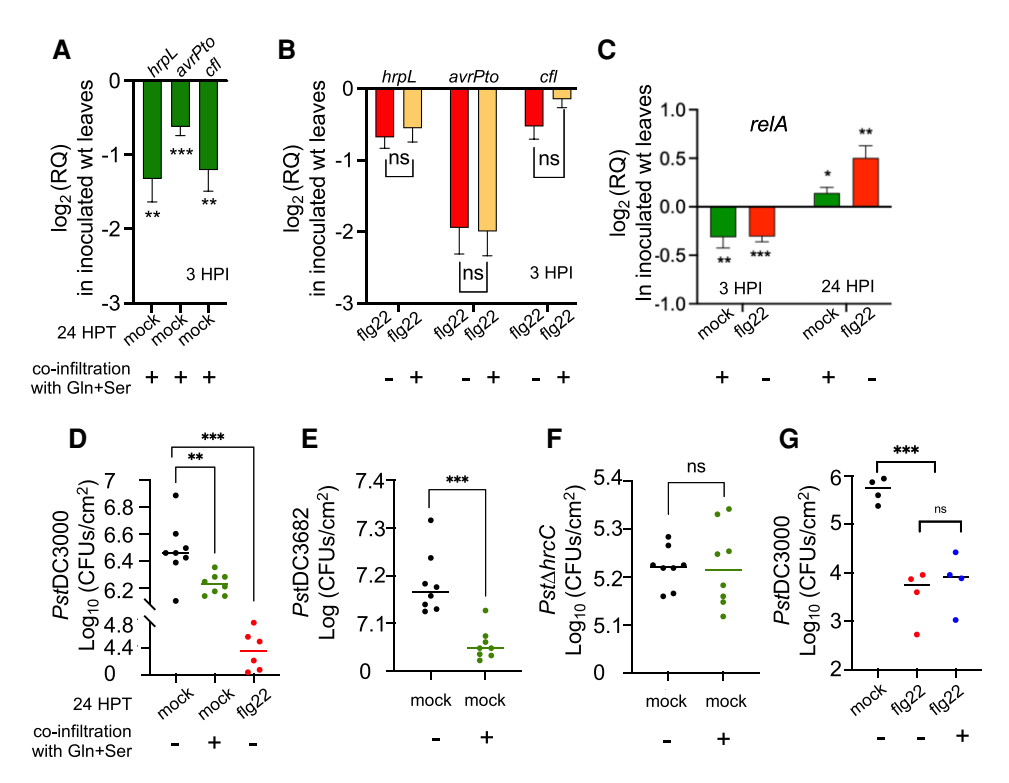
Figure 2. Amino acids that accumulate in MTI-elicited leaves modulate PstDC3000 growth and virulence in naïve wild-type plants. A) Bacterial growth 48 hours post-inoculation (HPI) of PstDC3000 alone (mock) or co-infiltrated with individual amino acids in leaves of naïve plants and normalized by the growth of PstDC3000 in mock. The number of plants used per condition is indicated atop. B) hrpL gene expression 2.5 h after inoculation of liquid HMM medium with PstDC3000 supplemented with the indicated amino acids and normalized by the expression in non-supplemented HMM medium. C) Expression of virulence genes in leaves of naïve plants 3 HPI with PstDC3000 co-infiltrated with either Gln (n = 12), Ser (n = 12), or Val (n = 18), normalized by the expression in non-supplemented PstDC3000. Statistical analysis: Brown-Forsythe and Welch ANOVA tests compared with mock (A); P values ≤ 0.05 (*), ≤ 0.01 (**), ≤ 0.001 (***) were adjusted by the two-stage step-up false discovery rate method (Q = 0.01). The center line indicates the median; the box extends from the 25th to 75th percentiles, and the whiskers show the entire data distribution. One sample t-tests for (B-D). Combined data of 3 (A,C) and 4 (B) independent experiments.

or Ser could prime plants for defense responses. In addition, CYP81F2 showed modest but significantly higher expression in leaves infiltrated with PstDC3000 and Gln + Ser compared to leaves infiltrated with PstDC3000 alone (Supplemental Fig. S6A). Nevertheless, when Gln + Ser were co-infiltrated with PstDC3000 into leaves of naïve plants, ICS1 and PR1 were expressed at the same level as those detected in leaves infiltrated with bacteria alone (Supplemental Fig. S6B). These data show that Gln and Ser supplementation do not suppress bacterial growth by eliciting plant defense responses.

The induced expression of CYP81F2 in leaves co-infiltrated with PstDC3000 and Gln + Ser likely reflects the virulencesuppressing effect of Gln + Ser on PstDC3000. MAMP perception strongly induces CYP81F2 and callose deposition, 2 responses that PstDC3000 suppresses early in the infection (Clay et al. 2009). These data suggest that Gln + Ser supplementation could impair the ability of PstD3000 to suppress early MAMP-elicited responses. To test this hypothesis, we examined hrpL gene expression, a major T3SS regulator in PstDC3000. Following the conditions established in an early study (Rahme et al. 1992), we grew PstDC3000 in hrpL-inducing minimal medium (HMM) supplemented with 5 mM of each L-AA for 150 min before collecting bacterial samples to assess gene expression. Except for Phe, every L-AA tested decreased hrpL expression in vitro, with Gln and Ser showing a large and statistically significant effect (Fig. 2B). It has been proposed that MAMPs perception elevates plant immunity against PstDC3000 via compromising the onset of bacterial virulence (Anderson et al. 2014; Lovelace et al. 2018; Nobori et al. 2018). To assess the impact of L-AA on bacterial virulence in planta, we tested the effect of Gln, Ser, Val, and His supplementation on virulence gene expression at early stages postinoculation. To this end, we co-infiltrated PstDC3000 with His, Gln, Ser, and Val individually in naïve

plants and assessed the expression of the T3SS regulator hrpL, the T3E avrPto, and the COR synthesis gene cfl. These 3 bacterial genes are induced at the early stages of the infection and have been used as virulence markers in previous studies (Lovelace et al. 2018; Nobori et al. 2018). While Gln and Ser significantly suppressed the expression of hrpL, avrPto, and cfl, Val only suppressed hrpL, avrPto (Fig. 2C). The co-infiltration of PstDC3000 with His did not affect the expression of these genes (Supplemental Fig. S7), suggesting that His boosts bacterial growth without modifying bacterial virulence. As a comparison, we tested the effect of citric acid, aspartic acid, and 4-benzoic acid on bacterial growth at 50 and 500 µM concentrations as previously reported by Anderson et al. (2014) in seedlings. Our data revealed that the 500 µM combination of the 3 metabolites modestly increased bacterial growth in mock-treated leaves but had no effect on bacterial growth in flg22-treated leaves (Supplemental Fig. S8A). In addition, these metabolites did not affect the expression of T3SS in mock- or flg22-treated plants, suggesting that, unlike in seedlings, these metabolites do not induce virulence and bacterial growth in planta (Supplemental Fig. S8B). Overall, our data suggest that Gln and Ser may play an important role in suppressing bacterial virulence gene expression in flg22-treated plants.

Although effective at suppressing bacterial growth and virulence gene expression, the surge in amino acid concentrations is only 1 of the many responses elicited after flg22 perception. To compare the virulence-suppressing activity of Gln + Ser with that of flg22 pretreated plants, we coinfiltrated *PstDC3000* with Gln + Ser in naïve wild-type plants or infiltrated *PstDC3000* alone in flg22 pretreated plants, and assessed the expression of the *hrpL*, *avrPto*, and *cfl*. While the expression of virulence genes was significantly lower in *PstDC3000* co-infiltrated with Gln + Ser compared



to *PstDC3000* infiltrated alone in naïve plants (Fig. 3A), these genes were expressed to similarly low levels in flg22-treated plants with or without Gln + Ser co-infiltration (Fig. 3B). Importantly, both Gln + Ser infiltration in naïve plants and flg22 pretreated plants suppressed the expression of *PstDC3000* virulence genes to a similar extent, suggesting that MTI suppresses bacterial virulence through the virulence-suppressing activity of Gln and Ser.

To explore potential mechanistic connections between L-AA availability and *Pst*DC3000 virulence suppression, we tested the expression of *relA*, a bacterial gene that controls the onset of survival and virulence programs in response to nutrient starvation (Traxler et al. 2008). *relA* encodes an enzyme that controls the intracellular levels of the signaling metabolite guanosine penta- and tetra-phosphate, collectively known as (p)ppGpp. Like in other bacterial species, *Pst*DC3000 expressed *relA* in a nitrogen-poor medium to higher levels than in a rich medium (Supplemental Fig. S9). When co-infiltrated with Gln + Ser, *Pst*DC3000 expressed lower levels of *relA* than when infiltrated alone in naïve plants 3 HPI (Fig. 3C). Twenty-four HPI, however, *Pst*DC3000 expressed higher levels of *relA* when co-infiltrated with Gln +

Ser in naïve plants or infiltrated alone in flg22-treated plants (Fig. 3C). These data suggest that the extra availability of Gln and Ser in the early stages of leaf colonization suppresses relA expression, likely compromising the early onset of bacterial virulence. At later stages in leaf colonization, a higher expression of relA may be necessary to withstand the harsher apoplastic environment encountered by bacteria that were compromised to suppress plant immunity earlier during the infection. To assess the contribution of Gln + Ser to MTI-mediated suppression of bacterial growth, we tested the growth of PstDC3000 co-infiltrated with Gln + Ser in naïve plants side by side with PstDC3000 inoculated alone in flg22-treated plants. Plants pretreated with flg22 24 h prior to bacterial inoculation suppressed bacterial growth to a larger extent than naïve plants co-infiltrated with PstDC3000 and Gln + Ser, suggesting that beyond Gln and Ser accumulation, other defense responses elicited by flg22 contribute to suppressing bacterial growth (Fig. 3D). Like PstDC3000, the growth of the COR synthesis mutant strain PstDC3682 was also suppressed when co-infiltrated with Gln + Ser (Fig. 3E). Unlike PstDC3000, however, the growth of the T3SS mutant strain $\Delta hrcC$ was similarly compromised in

L-AA-supplemented and nonsupplemented leaves (Fig. 3F), suggesting that Gln + Ser supplementation suppresses bacterial growth primarily via suppressing the expression of the T3SS. In addition, flg22 pretreated plants suppressed the growth of PstDC3000 to the same extent regardless of whether bacteria were infiltrated alone or co-infiltrated with Gln + Ser (Fig. 3G). The nonadditive effect of Gln + Ser supplementation on flg22-elicited bacterial growth suppression further supports the hypothesis that MTI suppresses bacterial virulence via increasing Gln and Ser availability. The relatively small protection conferred by Gln + Ser compared to MTI elicitation with flg22, indicates that additional defense mechanisms, elicited by flg22 and not by Gln and Ser, also contribute to suppressing bacterial growth. In support of the direct effect of Gln + Ser on PstDC3000, the coinfiltration of PstDC3000 with Gln + Ser in leaves of naïve fls2 plants bypassed the need for flg22 perception to suppress hrpL and cfl expression (Supplemental Fig. S10A) and bacterial growth (Supplemental Fig. S10B). Overall, our data show that Gln + Ser supplementation does not elicit plant defense responses and that the expression of bacterial virulence is significantly lower than control levels when PstDC3000 is coinfiltrated with Gln + Ser in planta. These data suggest that increased L-AA concentrations contribute to bacterial growth suppression directly by suppressing virulence.

SA signaling contributes to the accumulation of amino acids in MAMP-elicited leaves

The Arabidopsis SA-induced deficient-2 (sid2) mutant is a loss-of-function mutant of ICS1 that does not induce the synthesis of SA in response to microbial attack, a phenotype associated with attenuated responses to flg22 perception and enhanced susceptibility to PstDC3000 infections (Wildermuth et al. 2001; Tsuda et al. 2008). SA signaling has been shown to positively regulate the expression of AA/H⁺ symporters and the uptake activity in flg22-treated seedlings (Zhang et al. 2022). To test if SA could play a similar

role in plants, we assessed the expression of AA/H⁺ symporters in flg22-infiltrated leaves of wild-type and sid2 plants 8 HPT. Like in seedlings, while leaves of wild-type plants responded to flg22 perception by inducing the expression of several transporters, sid2 only partially induced these genes (Supplemental Fig. S11), suggesting that, like in seedlings, SA plays an important signaling role in L-AA transport in plants. Since SA is an important mediator of MAMP-elicited signaling and L-AA transport, we hypothesized that SA could also play an important role in the accumulation of L-AA in flg22-treated leaves. To test this hypothesis, we assessed the concentration of total L-AA in whole leaves and the leaf AWF of wild-type and sid2 plants 24 HPT with flg22. While leaf L-AA concentrations remained the same 24 HPT with water or flg22 (Fig. 4A), a modest increase in L-AA concentration, lower than that observed in the wild-type, was detected in the leaf AWF of flg22-treated sid2 plants (Fig. 4B), suggesting that SA-mediated signaling is required for leaves to accumulate L-AA in response to flg22 perception. As revealed by LC-MS analysis of sid2 AWFs (Supplemental Table S1), an increase in alanine seems to account for the modest increase of total L-AAs in response to flg22 perception (Fig. 4B). To test for potential connections between MAMP perception, SA-mediated L-AA accumulation, and bacterial virulence suppression, we tested if flg22-treated sid2 plants could suppress PstDC3000 virulence gene expression to a similar extent as wild-type plants. While flg22-pretreated wild-type plants significantly suppressed hrpL expression as early as 1 HPI, sid2 plants allowed PstDC3000 to express hrpL to a similar extent as mocktreated sid2 plants (Fig. 4C). By 3 HPI, however, flg22-pretreated sid2 plants suppressed the expression of hrpL to the same extent as flg22-pretreated wild-type plants (Fig. 4C). These data suggest that the compromised increase in L-AA concentrations in response to flg22 perception causes a delay in suppressing virulence gene expression in sid2. To address the contribution of increased L-AA levels

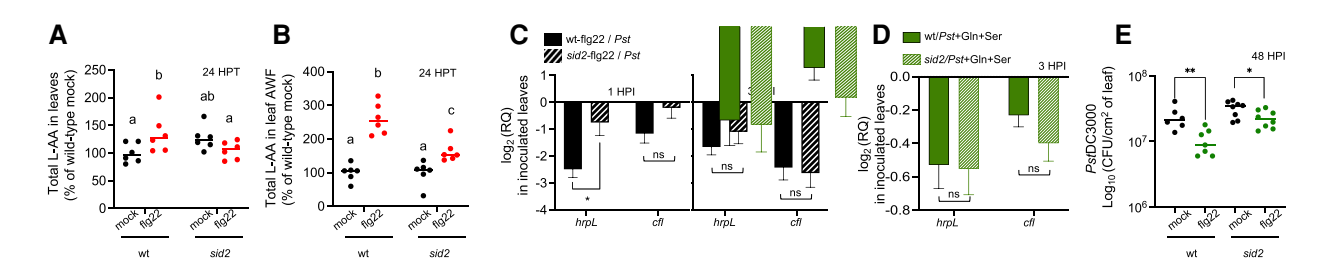


Figure 4. SA-mediated signaling contributes to the flg22-induced accumulation of L-AA and bacterial virulence suppression. A) Total L-AA in mock or flg22-treated leaves of wild-type (wt) or sid2-2 (sid2) plants 24 hours post-treatment (HPT). B) Total L-AA in leaf apoplastic washing fluids (AWF) of mock or flg22-treated wt or sid2 naïve plants 24 HPT. C) Expression of virulence genes in wt or sid2 flg22-treated plants inoculated with PstDC3000 alone and normalized by gene expression in mock-treated plants 1h or 3h post-inoculation (HPI); Mean \pm SEM (n = 3); D) Expression of virulence genes in wt or sid2 naïve plants co-infiltrated with PstDC3000 and Gln + Ser; Mean \pm SEM (n = 12). E) Bacterial growth in wt or sid2 naïve plants 48 HPI with PstDC3000 alone or PstDC3000 and Gln + Ser. Statistical analysis: one-way ANOVA (A,B); t-test (C-E). (A-E) one representative experiment from at least 3 independent experiments. (D) combination of 3 independent experiments. Different letters denote atop data denote statistically significant differences at P values ≤ 0.05 (*), ≤ 0.01 (***), ≤ 0.001 (***), or non-significant (ns) are shown (C-E).

on bacterial virulence and growth independently of SA-mediated defense, we bypassed SA signaling by coinfiltrating PstDC3000 with Gln + Ser in sid2 plants. Like in naïve wild-type plants, PstDC3000 co-infiltrated with Gln + Ser expressed similarly low levels of hrpL and cfl in naïve sid2 plants 3 HPI (Fig. 4D). In addition, the co-infiltration of PstDC3000 with Gln + Ser significantly suppressed bacterial growth in naïve sid2 plants albeit to a lower extent than in wild-type plants (Fig. 4E). While Gln + Ser co-infiltration suppressed bacterial growth in the SA-competent fls2 receptor mutant and wild-type plants to the same extent (Supplemental Fig. S10), the growth suppression was less pronounced in sid2 (Fig. 4E), suggesting that, besides suppressing virulence gene expression at early time points during leaf colonization, SA-mediated defense responses that operate at later time points contribute to suppressing bacterial growth all along the 48 h infection period. In addition, these data suggest that SA-mediated signaling positively regulates the accumulation of L-AA in flg22-treated leaves, thus suppressing bacterial virulence at early time points after inoculation.

High endogenous apoplastic Gln suppresses bacterial infections

To better mimic the high L-AA concentrations of MTI-elicited leaves without supplementing PstDC3000 with exogenous L-AA, we sought to assess the impact of high Gln concentrations on bacterial infections in leaves of naïve plants that constitutively accumulate high concentrations of L-AA in the leaf apoplast. The Arabidopsis GLUTAMINE DUMPER-1 gene encodes a transmembrane protein that positively regulates the secretion of Gln to the leaf apoplast. The gain-of-function mutant gdu1-1D constitutively accumulates high concentrations of Gln in the leaf apoplast (Pilot et al. 2004; Pratelli et al. 2010). While 0.8 mM Gln

concentrations are found in AWF of soil-grown gdu1-1D (Pilot et al. 2004), in pellet-grown gdu1-1D accumulated approximately 0.5 mM Gln compared to 0.3 mM in wild-type naïve plants (Supplemental Fig. S12). The constitutive secretion of Gln in gdu1-1D depletes cells from intracellular Gln and generates oxidative stress, followed by the accumulation of high concentrations of SA, spontaneous cell-death lesions, and the development of enhanced disease-resistance phenotype 4 wk after germination (Liu et al. 2010). To eliminate the SA-associated phenotypes that would otherwise make gdu1-1D unsuitable to test the role of high apoplastic Gln levels on bacterial gene expression and growth, we used the double mutant sid2×gdu1-1D that accumulates high Gln levels in the leaf apoplast without exhibiting any of the enhanced defense responses associated with SA accumulation (Liu et al. 2010). The double mutant accumulated higher amounts of L-AA in the leaf apoplast than wild-type and sid2 naïve plants (Fig. 5A). In naïve sid2×gdu1-1D plants, nonsupplemented PstDC3000 bacteria expressed hrpL, AvrPto, and cfl to lower levels than in sid2 plants (Fig. 5B). This result was reminiscent of the lower expression of these virulence genes in naïve wild-type or sid2 plants when PstDC3000 was co-infiltrated with Gln + Ser (Fig. 3A). In addition, and consistently with previous results obtained with Gln + Ser supplemented PstDC3000, bacterial growth was significantly lower in sid2×gdu1-1D compared to sid2 naïve plants (Fig. 5C). Altogether, these data demonstrate that Gln + Ser supplementation and high endogenous Gln concentrations similarly suppress PstDC3000 virulence and growth. The data also highlights the role of SA signaling in controlling L-AA levels in response to flg22 perception and provides a mechanistic explanation to understand the enhanced susceptibility to PstDC3000 infections of Arabidopsis mutants compromised for SA biosynthesis and signaling.

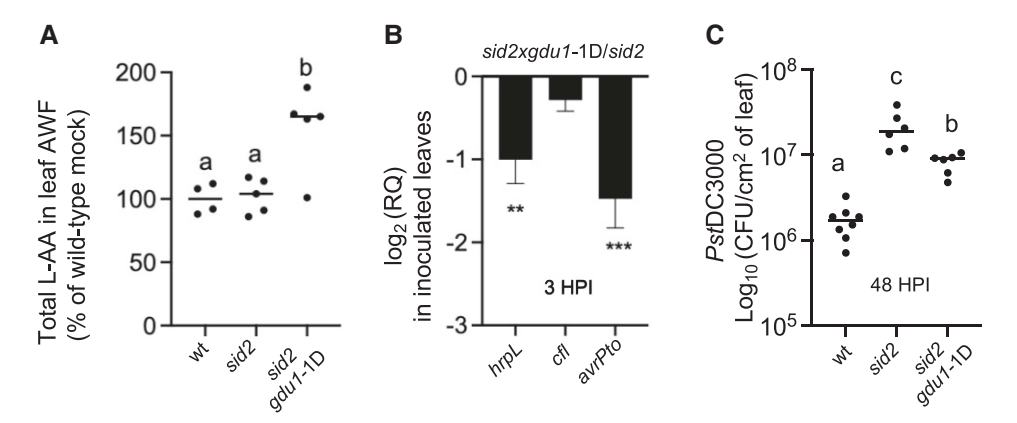


Figure 5. High endogenous levels of Gln impact PstDC3000 virulence and growth in naïve plants. A) Concentration of total amino acids (L-AA) in leaf apoplastic washing fluids (AWF) of wild-type (wt), sid2, and $sid2 \times gdu1$ -1D naïve plants. B) Expression of virulence genes in $sid2 \times gdu1$ -1D (n = 15) naïve plants inoculated with PstDC3000 alone and normalized by the expression in sid2 plants (n = 13); Mean \pm SEM C) PstDC3000 growth in wt, sid2, and $sid2 \times gdu1$ -1D naïve plants 48 HPl. Statistical analysis: Brown-Forsythe and Welch ANOVA tests (A) and (C); P values were adjusted by the two-stage step-up false discovery rate method (Q = 0.01). (A,C) one representative experiment from at least three independent experiments. (B) combination of 3 independent experiments. Different letters atop each data group denote statistically significant differences at P values ≤ 0.01 (**) and ≤ 0.001 (***) are shown in (B).

Discussion

Increased availability of amino acids in leaf apoplast suppresses the onset of bacterial virulence

Plant bacterial pathogens must sense the environment and activate virulence pathways to suppress induced plant defense before they can colonize the leaf apoplast (Xin et al. 2018). While low levels of virulence may hinder bacteria's ability to suppress plant defense responses, high levels of virulence expression may compromise bacterial growth by diverting energy away from the central metabolism (Xin et al. 2018). In most bacterial species, survival and growth are coordinated by the intracellular concentrations of (p) ppGpp (Traxler et al. 2008). In nitrogen-limiting, or otherwise suboptimal growth conditions (e.g. oxidative stress and osmotic stress) such as those experienced in minimal medium, bacteria express high levels of the (p)ppGpp-synthesis genes relA, thus allowing (p)ppGpp to accumulate. In turn, (p) ppGpp binds RNA polymerases, shifting transcription toward genes that are essential for virulence and stress survival. In the leaf apoplast, the availability of L-AA and other sources of carbon and nitrogen changes as the infection progresses, demanding PstDC3000 to constantly adjust (p)ppGpp levels to maximize growth. Upon entering the leaf apoplast, PstDC3000 spends the first 3 to 6 h sensing the new environment and adjusting its metabolism to express virulence genes in preparation for the rapid growth that takes place later in the infection (Nobori et al. 2018; Xin et al. 2018). In the early stages of host colonization, the main function of the T3SS is to suppress plant defense responses that would otherwise terminate the infection. Indeed, PstDC3000 mutants compromised to express a functional T3SS, elicit strong MTI and fail to infect otherwise susceptible host plants (Hauck et al. 2003). Similarly, PstDC3000 mutant strains compromised for the synthesis of (p)ppGpp, are unable to express wild-type levels of T3E proteins and only produce modest infections in otherwise susceptible Arabidopsis plants (Chatnaparat et al. 2015a, 2015b). The early expression of the T3SS has been proposed as an important factor to predict the success of PstDC3000 to produce infections (Nobori et al. 2018). In agreement with previous studies, our data show that 3 HPI in MTI-elicited plants, PstDC3000 expresses levels of relA and virulence genes lower than those detected in naïve plants. The low expression of relA in MTI-elicited plants is consistent with the metabolic adjustment to the nitrogen-rich leaf apoplast environment provided by plants that have accumulated L-AA prior to the inoculation (Fig. 1, Table 1, Fig. 3, B and C). Similarly, PstDC3000 expresses low levels of relA and virulence genes when co-infiltrated with Gln + Ser into naïve wild-type plants (Fig. 2, Fig. 3, A and C), again suggesting that high Gln + Ser concentrations, such as those encountered when infiltrated in leaves of MTI-elicited plants, serve a passive defensive function aimed at lowering bacterial stress responses and virulence. Twenty-four HPI, however, PstDC3000 coinfiltrated with Gln + Ser in naïve plants, or infiltrated alone in MTI-elicited plants, expressed higher levels of *relA* compared to bacteria infiltrated alone in naïve plants (Fig. 3C). These data suggest that *PstDC3000* experiences a higher level of stress at later time points when co-infiltrated with Gln + Ser in naïve plants, perhaps due to not having been able to suppress plant defense responses earlier in the infection (Fig. 3, A and C). Importantly, *PstDC3000* expressed similarly low levels of T3SS, T3E, and COR biosynthesis genes when infiltrated alone into leaves of flg22-treated plants (Fig. 3A) or when co-infiltrated with Gln + Ser into naïve plants (Fig. 3B), suggesting that Gln + Ser and flg22 pretreatment suppress bacterial virulence gene expression through similar mechanisms.

Amino acid-mediated suppression of virulence only partially suppresses bacterial growth

MTI suppresses not only the growth of the virulent PstDC3000 wild-type strain but also that of T3SS mutants that typically produce mild infection in wild-type naïve Arabidopsis plants, suggesting that other mechanisms beyond T3SS suppression may account for MTI-mediated protection against bacterial infections (Nobori et al. 2018). This evidence is consistent with the suppressing activity that Gln + Ser exerts on PstDC3000 growth described in this study. L-AA supplementation in naïve plants did not suppress PstDC3000 growth to the same extent as MTI-elicited plants (Fig. 3E). In addition, although effective at suppressing the growth of bacterial strains that do not produce COR (Fig. 3F), L-AA supplementation did not suppress the growth of the $\Delta hrcC$ strain (Fig. 3G). These data suggest that the increased availability of amino acids elicited by flg22 in wild-type plants suffices to suppress bacteria virulence, but it is insufficient to suppress bacterial growth fully. This model is consistent with L-AA playing a defensive role in suppressing virulence, a critical mechanism in the early stages of infection, but implies that other offensive responses are needed to further restrict bacterial growth in MTI-elicited plants. This hypothesis is supported by the fact that, while Gln + Ser supplementation suppressed bacterial virulence similarly in wild-type and sid2 plants (Fig. 4D), they only partially suppressed bacterial growth in sid2 compared to wild-type plants (Fig. 4E). In addition, while the expression of virulence genes is suppressed to a greater extent in sid2×gdu1-1D than in sid2 (Fig. 5B), the enhanced disease susceptibility phenotype of sid2 was only partially rescued by the increased availability of Gln in the sid2×gdu1-1D background (Fig. 5D). These data demonstrate that beyond the early suppression of virulence, active defense mechanisms mediated by SA signaling restrict bacterial growth as the infection progresses. Hence, we propose that the bacterial infection level observed 48 HPI depends on both, defensive responses that suppress virulence within the first 3 HPI and offensive responses that create a harsher environment as bacteria continue to colonize the leaf apoplast.

SA signaling positively regulates the accumulation of amino acids in response to MAMPs perception

SA regulates defense responses against biotrophic and hemibiotrophic pathogens at multiple levels. In addition to playing an essential role in activating cell-death-mediated resistance initiated by plant intracellular receptors that detect bacterial T3E, SA plays a critical role in activating immunity upon MAMP perception (Tsuda et al. 2008). In a previous study, we unveiled that SA plays a positive role in regulating the basal update and the enhanced uptake of L-AA elicited by MAMPs perception in Arabidopsis seedlings (Zhang et al. 2022). Like in seedlings, SA is necessary to induce the expression of AA/H⁺ symporters in response to MAMP perception in mature leaves of plants (Supplemental Fig. S9) (Zhang et al. 2022). The biological function of the induced gene expression and enhanced L-AA uptake activity detected in seedlings is still unclear. One possibility is that the enhanced uptake lowers the concentrations of L-AA in the leaf apoplast and deprives PstDC3000 of carbon and nitrogen at the late stages of infection. In support of this possibility, the expression of relA, a bacterial proxy for nitrogen scarcity, was higher in PstDC3000 infiltrated into MTI-elicited plants than in mock-treated plants 24 HPI (Fig. 3C). The late induction of relA (e.g. 24 HPI) in wild-type plants likely induces the onset of bacterial survival programs, diverting energy away from central metabolism and perhaps further compromising bacterial growth. Since sid2 plants accumulate less L-AA than wild-type plants in the leaf apoplast (Fig. 4B) and take up less L-AA in response to flg22 treatment in the seedlings stage (Zhang et al. 2022), we hypothesize that the SA-dependent uptake of L-AA contributes to lowering apoplastic L-AA levels at late infection stages. Overall, the evidence collected in this study and our previous study suggests that SA signaling is needed for the PAMP-induced fast increase in L-AA concentrations in the apoplastic side of the plasma membrane, which suppresses the onset of bacterial virulence at early infection stages. Such virulence suppression likely provides plants with time to mount offensive responses without bacterial interference. At later time points, SA signaling is required to induce L-AA transporters that will enhance the uptake of L-AA and likely deprive bacteria of the carbon and nitrogen needed to support rapid growth.

How amino acids suppress bacterial virulence during MTI

A simplified model of bacterial virulence suppression is presented in Supplemental Fig. S13. When plants perceive MAMPs and mount defense responses in the absence of bacterial interference, the series of events that follow recapitulate the sequence of events elicited by nonpathogenic bacterial strains: the plant cells perceive the incoming bacteria and quickly elicit the accumulation of free amino acids in the leaf apoplast, which prevents bacterial from expressing virulence. Data obtained in a previous study showed that the perception of flg22 and elf26 quickly inhibits the

uptake of L-AA within the first 4 HPT in Arabidopsis seedlings (Zhang et al. 2022). Since the uptake of L-AA is mediated by AA/H⁺ symporters whose activity depends on the H⁺ gradient across the plasma membrane, we hypothesized that the inhibition of L-AA uptake observed within the first hours after flg22 or elf26 perception (Zhang et al. 2022) could result from the inhibition of the H⁺-pump ATPase AHA1 and the rapid change in ion fluxes across the plasma membrane that combined leads to the alkalinization of the apoplastic fluids (Jeworutzki et al. 2010; Elmore and Coaker 2011). In liquid-grown seedlings and liquid-cultured plant cells, the alkalinization of the liquid medium is one of the first responses elicited by fungal ergosterol (Granado et al. 1995), flg22 (Felix et al. 1999), and a shorter version of the elf26 peptide called elf18 (Kunze et al. 2004), among other MAMPs. Due to technical limitations, the alkalinization of the leaf apoplastic fluids has yet to be confirmed in the leaves of intact plants. In addition, technical limitations hinder the direct assessment of L-AA transport activity in intact leaves. Thus, we can only infer that flg22 perception in plants inhibits the L-AA uptake activity via the alkalinization of the leaf apoplast. Notwithstanding the lack of direct evidence in planta, we have demonstrated that flg22 and elf26 perception also inhibit the uptake of L-AA in protoplasts of mesophyll cells obtained from plants (Zhang et al. 2022), suggesting that a similar inhibition of L-AA uptake may occur in the mesophyll cells of intact leaves. The combined action of passive L-AA secretion from mesophyll cells and the inhibition of active L-AA uptake would likely result in a net increase in L-AA levels on the apoplastic side of the plasma membrane. However, it is still unknown if the net increase in L-AA concentrations in the leaf apoplast elicited by flg22 perception 24 HPT (Fig. 1C) results from the inhibition of L-AA uptake. Like in seedlings, the induction of AA/H⁺ symporters elicited by flg22 in leaves would seem to indicate that an enhanced uptake, similar to that observed in seedlings (Zhang et al. 2022) would take place in intact leaves as soon as the early inhibition of uptake subsides. Further studies will be necessary to understand if and how the inhibition of L-AA uptake contributes to rapidly increasing L-AA concentration in flg22-treated intact leaves, as well as the identity of the transporters that allow L-AA to accumulate in the leaf apoplast.

Materials and methods

Plant growth conditions

Arabidopsis (A. thaliana) plants were grown on pellets (Jiffy Pellets #7) in growth Conviron Gen100 chambers with 9 h of light photoperiod, 100 μ E.m⁻².s⁻¹ light energy, 23 °C, and 70% relative humidity (RH). Plants were watered with half-strength Hoagland solution 3 times a week for the first 4 wk. Then, plants were watered with tap water 3 times a week for 2 more weeks. Wild-type plants were the reference Col-0 ecotype unless otherwise specified. The *sid2* mutant

(sid2-2 allele) was a gift from Mary Wildermuth at the University of California Berkeley. The gdu1-1D mutant was identified in an activation-tagged screen as described in Pilot et al. (2004). Seedlings were grown in liquid Murashige and Skoog (MS) basal medium with vitamins (Phytotechnology Laboratories) supplemented with 0.5 g/L MES hydrate and 5 g/L sucrose, pH 5.7 corrected with KOH, in a Conviron Adaptis A1000 growth chambers (Conviron, Inc.) under 16 h of light photoperiod, 23 °C constant temperature, 100 μE.m⁻².s⁻¹ light energy, and 80% RH.

Extraction and quantification of amino acids with fluorometric assay

The 4th and 5th pairs of leaves were collected in 2 ml roundbottom microcentrifuge tubes and flash-frozen at the indicated time points (see figure legends) after infiltration. For seedlings, $1 \mu M$ flg22 of the synthetic (QRLSTGSRINSAKDDAAGLQIA; GenScript, Cat# RP19986) was added on Day 10, and 24 h later samples were flashfrozen in liquid nitrogen. Frozen leaf and seedling samples were then lyophilized and weighed. The dry weight was adjusted to approximately 11 mg in each sample and turned into powder with two 5 mm stainless steel beads with Qiagen Tissue Lyser for 5 min at 3000 strokes per minute. Extraction in 400 µl of 80% v/v methanol was performed by mixing thoroughly with Qiagen Tissue Lyser for 5 min at 3000 strokes per minute. The samples were incubated at 28 °C overnight, centrifuged at 17.000 x g for 10, and 300 µl of the supernatant were transferred to a new tube and mixed with 200 µl of chloroform and 100 µl of water. The samples were mixed with a Qiagen Tissue Lyser for 1 min at 3000 strokes per minute and then centrifuged at $17.000 \times g$ for 10 min. The clear upper phase (150 µl) was transferred to a new tube for air drying and resuspended in HPLC-grade water. Apoplastic washing fluids were obtained using the infiltration and centrifugation method (Lohaus et al 2001). The 4th and 5th pairs of leaves were infiltrated with water or 1 µM flg22 as described above. Twenty-four hours postinfiltration, the leaves from 2 plants (8 leaves total) were pooled together as 1 sample and rolled together to fit inside the cylinder of a 5 ml sterile syringe. The tip of the syringe was sealed with parafilm, the leaves inside the cylinder were submerged in sterile water, the plunger was inserted in the cylinder, and the leaves were infiltrated by repeatedly applying positive and negative pressure by gently moving the plunger up and down. Once fully infiltrated, the leaves were removed from the syringe and pat-dried on tissue paper to remove surface water. Leaves of each sample were stacked together and inserted back in the cylinder of a clean 5 ml syringe without a plunger. The syringe was inserted in a clean 15 ml conical tube and centrifuged for 5 min at $500 \times g$ in a swinging bucket clinical centrifuge. Apoplastic washing fluids were collected at the bottom of the 15 ml conical tube, transferred to 1.5 ml microcentrifuge tubes, and stored at -80 °C until analysis. Phloem sap was collected as

described by Corbesier et al. (2002) with minor modifications. Briefly, previously infiltrated leaves were detached from the plant at the base of the petioles and rinsed in 10 mM EDTA to remove cellular content at the edge of the cut. Petioles ends were then submerged in 400 µl of 5 mM EDTA at 100% RH for 6 h in the dark at 23 °C. Phloem sap samples diluted in EDTA were then lyophilized and stored at room temp.

Free amino acids were quantified with the commercial L-AA (total AA) or the Gln fluorometric assay kits (BioVision, Inc; Cat # K639 and Cat# K556) following the manufacturer's directions. Briefly, a 12.5 µl reaction mix containing 11.5 µl L-AA assay buffer, 0.5 µl L-AA probe, and 0.5 µl L-AA enzyme mix was added to each well containing 12.5 µl of AWFs or L-AA standards to generate a standard curve. The reactions were incubated in a microtiter plate reader (SpectraMax® i3x, Molecular Devices) for 30 min at 37 °C. The fluorescent signal ($E_x/E_m = 535/587 \text{ nm}$) in each well was recorded every 5 min. AA quantification was performed on 5 to 6 independent samples per condition. Total amino acid concentration in each sample was calculated using the TREND function in excel and the standard calibration curve.

Profiling of amino acids leaf tissue

Fourth and fifth pairs of leaves were infiltrated with water or 1 µM flg22 for 24 h before being collected in 2 ml round bottom tubes and flash-frozen. Samples were then lyophilized and weighed. The dry weight of each sample was adjusted to approximately 5 mg. Dried leaves were crushed into powder with metal beads in a Qiagen Tissue Lyser. Amino acids were extracted with 200 µl of HCl 10 mM spiked with 0.1 mM Novarline (Sigma-Aldrich) as an internal extraction control, plus 200 µl of Chloroform. Each sample was vortexed for 2 min and centrifuged at 17,000 × g for 5 min. The supernatant was transferred to a new tube for analysis using a method previously described (Collakova et al. 2013). Briefly, samples were derivatized with AccQ•TagTM labeling fluorescence kit (Waters Corporation), and amino acids were separated using ultra-performance liquid-chromatography (UPLC) with an Acquity UPLC and detected using an Acquity FLP fluorescence detector (Waters Corporation).

Profiling of amino acids in apoplastic washing fluids

The quantification of individual amino acids in AWFs was performed at the University of Virginia-Biomolecular Analysis Facility Core following a standard protocol (Nemkov et al. 2015). Serial dilutions of standards of every AA were run for every analysis. Five microliters of samples were injected into a UHPLC system (Ultimate 3000, Thermo, San 378 Jose, CA, USA) and separated through a 3 min isocratic elution (5% v/v acetonitrile, 95% v/v water, 0.1% v/v formic acid) on a 1.7 μm C18 column (Kinetex XB-C18, Phenomenex, Torrance, CA, USA) at 250 µl/min and 25 °C. High-resolution mass spectrometry analysis was

performed using a triple quadrupole orbitrap mass spectrometer (Q-Exactive HF-X, Thermo Scientific).

Bacterial infection assays in Arabidopsis plants

Infections were performed as described previously by Hauck et al. (2003) with minor modifications. Plants were grown in pit pellets and watered as indicated above. Fully expanded leaves (4th and 5th pairs) of 6-wk-old plants were pressure infiltrated from the abaxial side of the leaf lamina with a sterile 1 ml needleless syringe loaded with bacterial suspension. PstDC3000 inoculum from -80 °C glycerol stock was streaked on an LB-agar plate and incubated overnight at 28 °C. A small amount of bacterial lawn from the overnight plate was transferred to 3 ml King's Broth media in a 50 ml conical tube and incubated under agitation for 3 to 4 h at 28 °C to an OD600nm of 0.4 to 0.7. Bacteria were pelleted by centrifugation at $8.000 \times g$ for 3 min and resuspended in sterile water. The pelleting and resuspension were repeated 3 times to wash the bacterial inoculum. Bacteria were resuspended in 5 mM MES buffer (pH 5.7), and the OD600nm was adjusted to 0.0002. For $Pst\Delta hrpC$ (T3SS mutant) and PstDC3682 (COR mutant), an OD_{600nm} of 0.02 was used for plant inoculation to compensate for the slow $Pst\Delta hrpC$ and PstDC3682 bacterial growth in wild-type Col-0 plants. Pst∆hrpC and PstDC3682 were provided by Prof. Alan Collmer (Cornell University) and Prof. Barbara Kunkel (University of Washington), respectively. For amino acids supplementation, each amino acid was added to the bacterial suspension to reach a 10 mM final concentration and immediately infiltrated into leaves. When combined, Gln and Ser were supplemented at 10 mM each. For the elicitation of MTI before bacterial inoculation, leaves were infiltrated with water (mock) or with 1 µM flg22 peptide via pressure infiltration (as described above) 24 h prior to bacterial inoculation. Infections were allowed to proceed for 48 h. For bacterial infection quantification, leaves were removed from the plants, and 5 mm in diameter leaf discs were collected with a hole puncher and transferred to 2 ml round bottom tubes. Samples were ground in 400 µl of sterile water with metal beads in a QIAGEN Tissue Lyser. Ten-fold serial dilutions of the ground leaf samples were plated on LB rifampicin 50 μg/ml Omin TrayTM single-well rectangular plates (NuncTM) and incubated overnight at 28 °C. Colony forming units (CFUs) were counted under the microscope (Olympus SZ61) and informed as CFUs per cm² of leaf area.

Bacterial virulence gene expression

PstDC3000 from an overnight liquid King's B culture was transferred to a sterile 50 ml conical tube with fresh media (1:10 dilution) and incubated at 28 °C for 2 h with agitation. For in vitro gene expression analysis, PstDC3000 was pelleted by centrifugation, washed 3 times with sterile water, and resuspended in Hrp-inducing minimal medium (Huynh et al. 1989). Bacteria were added to wells of a 12-well tissue culture plate at a final optical density (OD_{600nm}) of 0.2, and individual L-AAs were added at a 5 mM final concentration to the

corresponding wells by triplicate. The plates were incubated at room temperature (23 °C) for 150 to 190 min before the bacteria were transferred to microcentrifuge tubes, pelleted, and stored at -80 °C for RNA extraction. For in planta gene expression analysis, *Pst*DC3000 was resuspended at an OD_{600nm} of 0.2 in 5 mM MES (pH 5.7). For control experiments, *Pst*DC3000 was infiltrated into leaves as is. For amino acids supplementation experiments, bacteria were added to L-AAs solution prepared in 5 mM MES (pH 5.7) and immediately infiltrated into the 4th and 5th pairs of leaves. Leaf samples were taken between 150 and 180 min after infiltration, flash-frozen in liquid nitrogen, and stored at -80 °C for RNA extraction.

Bacterial growth in supplemented minimal medium

Bacteria were grown overnight in 5 ml of King's B liquid medium at 28 °C with shaking. Bacterial cultures were diluted 1:10 with fresh King's B medium the following morning; once the culture reached 0.5 OD_{600nm}, the bacteria were pelleted and resuspended in water 3 times. Washed bacteria were resuspended to a final OD600 of 0.05 in modified M9 media, containing KH₂PO₄ 15 g/L; NaCl 2.5 g/L; Na₂HPO₄ 33.9 g/L; NH₄Cl 5 g/L; MgSO₄ 5 mM, sucrose 100 μM, and supplemented with Gln, Ser or a combination of both. Bacteria were grown in 96 well plates with near constant agitation at 28 °C. OD_{600nm} measurements were taken every 2 min.

RNA extraction and RT-qPCR

Leaf samples or bacterial pellets were removed from the -80 °C freezer and kept on dry ice until grinding. Right before grinding, Trizol Reagent (Invitrogen) was added to each tube, and samples were ground with metal beads and a QIAGEN Tissue Lyser. For bacteria RNA extraction either from leaves or bacterial pellets, Trizol Reagent (Invitrogen) and 0.1 mm in diameter Zirconia/Silica beads (Sigma-Aldrich) were added to each tube and pulverized with a bead beater (BioSpec Products) for 2 min at 7.000 stroke/min before proceeding with RNA purification. RNA samples were then treated with DNAse-I (Promega) to remove genomic DNA contamination. cDNA was synthesized with M-MLV retrotranscriptase (Promega) and random hexamers primers (Invitrogen). RT-qPCR reactions were carried out with SYBR Green reagent (CoWin Biosciences, Inc.) in an BiosystemsTM Applied 7500 Fast Real-Time Instrument. Actin2 (At3g18780) expression and gyrA (PSPTO_1745) were used as normalizing housekeeping genes for Arabidopsis and PstDC3000, respectively. Gene expression data are shown as the logarithmic transformation of 2 (log₂) times 2 to the power of minus delta-delta Ct (2^{-ddCt}), a mathematical formulation that represents fold change gene expression as log₂ of relative quantification, or log₂ (RQ), for short. The sequences of the primers used were:

gyrA-F: 5'-ttcL-AAtgctgatcccggaagaagg-3'; gyrA-R: 5'-atttc ctcaccatccagcacctga-3';

hrpL-F: 5'-tcaggaaagctgggaagacgaagt-3'; hrpL-R: 5'-atgttcg acggcaggcaatcaatg-3';

avrPto-F: 5'-atgacgggagcgtcaggaatcaat-3'; avrPto-R: 5'-atcc gttcgggttcatagtcgcaa-3';

cfl-F: 5'-tgctcgtctcgtcgccaa-3'; cfl-R: 5'-cgatacccttagttagtcc

CYP81F2-F: 5'-ctcatgctcagtatgatgc-3'; CYP81F2-R: 5'-ctcca atcttctcgtctatc-3';

WRKY29-F: 5'-atccaacggatcaagagctg-3'; WRKY29-R: 5'-gcg tccgacaacagattctc-3';

ICS1-F: 5'-gaactcaaatctcaacctcc-3'; ICS1-R: 5'-actgcgacgag agaagaaac-3';

PR1-F: 5'-ttcttccctcgaaagctcaa-3'; PR1-R: 5'-aaggcccaccaga gtgtatg-3';

Gene expression analysis of Arabidopsis amino acid transporters

The 4th and 5th pairs of leaves of 6-wk-old plants were infiltrated with water (mock treatment) or 1 µM of flg22 synthetic peptide with a needleless syringe. Eight hours later, leaves were removed from plants, snap froze in liquid nitrogen, and the RNA samples were obtained with Trizol Reagent (Invitrogen). One microgram of total RNA per sample was used for nanoString hybridization with the probes listed in Supplemental Fig. S11B. Raw counts were analyzed with the nSolver® software (nanoString, Inc) to calculate fold change in gene expression described in Geiss et al. (2008).

Quantification of radiolabeled amino acids in whole leaf and leaf apoplastic washing fluids

Using a needleless 1 ml syringe, the 2nd and 3rd pair of leaves from 6-wk-old plants were infiltrated with a mix of 1 mM cold amino acids (Gln, Ser, or Pro) spiked with the corresponding ¹⁴C labeled amino acid. One hour after infiltration, the leaves were removed from the plants at the base of the lamina, quickly rinsed in water, and transferred to a 5 ml sterile syringe without a plunger. Apoplastic washing fluids were obtained as described above in the "Extraction and quantification of amino acids with fluorometric assay" section. After collecting apoplastic washing fluids, the leaves in each sample were transferred to a 2 ml round bottom microcentrifuge tube containing two 5 mm metal beads and 400 µl of 5% v/v bleach (to remove chlorophyll) and ground with the QIAGEN Tissue Lyser. The recovered apoplastic washing fluids, typically 100 µl, were mixed with 100 µl of scintillation cocktail and kept in the dark for 2 h. One hundred microliters of the leave's lysates were lyophilized overnight, resuspended in 100 µl of water, mixed with 100 µl of scintillation cocktail, and stored in the dark for 2 h. Radioactivity in each sample was assessed as counts per minute (CPMs) using a Wallac 1450 TriLux MicroBeta 96-well plate liquid scintillation counter (PerkinElmer).

Accession numbers

Sequence data from this article can be found in the GenBank data libraries under accession numbers NM_118486.6_

(WRKY29), NM 127025.3 (PR1); NM 202414.1 (ICS1); NM 119322.4 (GDU1); NM 125104.3 (CYP81F2); NM 0013383 58.1 (ACT2); gene ID 1183382 (PstDC3000 gyrA); gene ID: 1183040 (PstDC3000 hrpL); gene ID: 1186363 (PstDC3000 cfl); gene ID: 1185679 (PstDC3000 AvrPto); and gene ID: 947244 (relA). Accession numbers of Arabidopsis AA/H + symporters are shown in Supplemental Fig. S11.

Supplemental data

The following materials are available in the online version of this article.

Supplemental Table S1. Concentrations of individual amino acids in leaf AWF of wild-type and sid2 plants 24 h posttreatment with water (mock) or 1 µM flg22.

Supplemental Figure S1. Total amino acids in whole leaves of wild-type (wt) and fls2 plants infiltrated with water (black) or flg22 (red) 24 h posttreatment.

Supplemental Figure S2. Supplemented amino acids were quickly removed from the leaf apoplast.

Supplemental Figure S3. Gln + Ser supplementation suppresses PstDC3000 growth in planta.

Supplemental Figure S4. Gln and Ser supplementation promotes PstDC3000 growth in vitro.

Supplemental Figure S5. Gln + Ser supplementation does not affect bacterial titter at 3 h postinoculation.

Supplemental Figure S6. Arabidopsis defense gene expression in response to Gln + Ser infiltration.

Supplemental Figure S7. Expression of virulence genes in PstDC3000 co-infiltrated with 10 mM His in naïve plants 3 h postinoculation.

Supplemental Figure S8. Effect of citric acid, aspartic acid, and 4-benzoic (CAB) on PstDC3000 growth and virulence in 6-wk-old plants.

Supplemental Figure S9. relA expression in hrp-inducing minimal medium (HMM) normalized by its expression in King's B (KB) rich medium.

Supplemental Figure S10. Exogenous supplementation of Gln + Ser bypasses flg22 perception to suppress bacterial virulence in fls2.

Supplemental Figure S11. Amino acid transporters gene expression in flg22-infiltrated plants.

Supplemental Figure S12. High endogenous Gln level in the leaf apoplastic washing fluids of gdu1-1D.

Supplemental Figure S13. A tentative model of how plant-made amino acids suppress bacterial virulence during MTI.

Acknowledgments

To Frank Zhao at the University of Illinois for fruitful discussion on the early stages of this study. To members of the Danna lab, especially Renyu Li, Franco Rossi, and Patryk Puchalski, for their contributions to generating preliminary data for this study.

Author contributions

X.Z. and C.H.D. designed the experiments; X.Z., P.J.T., I.D.K.A., P.K., C.T., and C.D. performed experiments; X.Z., E.C., G.P., and C.H.D. analyzed the data. C.H.D. prepared figures and wrote the manuscript.

Funding

This work was supported by the National Science Foundation CAREER Award IOS-1943120 grant (to C.H.D.).

Conflict of interest statement. The authors declare no conflict of interest.

Data availability

All materials available upon request.

References

- **Abramovitch RB, Martin GB.** Strategies used by bacterial pathogens to suppress plant defenses. Curr Opin Plant Biol. 2004:**7**(4): 356–364. https://doi.org/10.1016/j.pbi.2004.05.002
- Adams-Phillips L, Briggs AG, Bent AF. Disruption of poly(ADP-ribosyl)ation mechanisms alters responses of Arabidopsis to biotic stress. Plant Physiol. 2009:152(1): 267–280. https://doi.org/10.1104/pp.109.148049
- Anderson JC, Wan Y, Kim YM, Pasa-Tolic L, Metz TO, Peck SC. Decreased abundance of type III secretion systeminducing signals in Arabidopsis mkp1 enhances resistance against *Pseudomonas syringae*. Proc Natl Acad Sci USA. 2014:**111**(18): 6846–6851. https://doi.org/10.1073/pnas.1403248111
- Asai T, Tena G, Plotnikova J, Willmann MR, Chiu WL, Gomez-Gomez L, Boller T, Ausubel FM, Sheen J. Map kinase signal-ling cascade in Arabidopsis innate immunity. Nature. 2002:415-(6875): 977–983. https://doi.org/10.1038/415977a
- Bender CL, Stone HE, Sims JJ, Cooksey DA. Reduced pathogen fitness of *Pseudomonas syringae* pv. Tomato Tn5 mutants defective in coronatine production. Physiol Mol Plant Pathol. 1987:**30**(2): 273–283. https://doi.org/10.1016/0885-5765(87)90040-3
- **Bigeard J, Colcombet J, Hirt H**. Signaling mechanisms in pattern-triggered immunity (PTI). Mol Plant. 2015:**8**(4): 521–539. https://doi.org/10.1016/j.molp.2014.12.022
- **Brooks DM, Bender CL, Kunkel BN**. The *Pseudomonas syringae* phytotoxin coronatine promotes virulence by overcoming salicylic acid-dependent defences in *Arabidopsis thaliana*. Mol Plant Pathol. 2005:**6**(6): 629–639. https://doi.org/10.1111/j.1364-3703.2005.00311.x
- Chatnaparat T, Li Z, Korban SS, Zhao Y. The bacterial alarmone (p) ppGpp is required for virulence and controls cell size and survival of *Pseudomonas syringae* on plants. Environ Microbiol. 2015a:17(11): 4253–4270. https://doi.org/10.1111/1462-2920.12744
- Chatnaparat T, Li Z, Korban SS, Zhao Y. The stringent response mediated by (p)ppGpp is required for virulence of *Pseudomonas syringae* pv. Tomato and its survival on tomato. Mol Plant-Microbe Interact. 2015b:28(7): 776–789. https://doi.org/10.1094/MPMI-11-14-0378-R
- Chezem WR, Memon A, Li F-S, Weng J-K, Clay NK. SG2-type R2R3-MYB transcription factor MYB15 controls defense-induced lignification and basal immunity in Arabidopsis. Plant Cell. 2017:29(8): 1907–1926. https://doi.org/10.1105/tpc.16.00954
- Clay NK, Adio AM, Denoux C, Jander G, Ausubel FM. Glucosinolate metabolites required for an Arabidopsis innate immune response.

- Science. 2009:**323**(5910): 95–101. https://doi.org/10.1126/science. 1164627
- Collakova E, Aghamirzaie D, Fang Y, Klumas C, Tabataba F, Kakumanu A, Myers E, Heath L, Grene R. Metabolic and transcriptional reprogramming in developing soybean (*Glycine max*) embryos. Metabolites. 2013:3(2): 347–372. https://doi.org/10.3390/metabo3020347
- Corbesier L, Bernier G, Périlleux C. C:N ratio increases in the phloem sap during floral transition of the long-day plants Sinapis alba and *Arabidopsis thaliana*. Plant Cell Physiol. 2002:**43**(6): 684–688. https://doi.org/10.1093/pcp/pcf071
- **Elmore JM, Coaker G**. The role of the plasma membrane H+-ATPase in plant–microbe interactions. Mol Plant. 2011:**4**(3): 416–427. https://doi.org/10.1093/mp/ssq083
- Felix G, Duran JD, Volko S, Boller T. Plants have a sensitive perception system for the most conserved domain of bacterial flagellin. Plant J. 1999:18(3): 265–276. https://doi.org/10.1046/j.1365-313X.1999. 00265.x
- Geiss GK, Bumgarner RE, Birditt B, Dahl T, Dowidar N, Dunaway DL, Fell HP, Ferree S, George RD, Grogan T, et al. Direct multiplexed measurement of gene expression with color-coded probe pairs. Nat Biotechnol. 2008:26(3): 317–325. https://doi.org/10.1038/nbt1385
- **Gómez-Gómez L, Felix G, Boller T**. A single locus determines sensitivity to bacterial flagellin in *Arabidopsis thaliana*. Plant J. 1999:**18**(3): 277–284. https://doi.org/10.1046/j.1365-313X.1999.00451.x
- Goto Y, Maki N, Ichihashi Y, Kitazawa D, Igarashi D, Kadota Y, Shirasu K. Exogenous treatment with glutamate induces immune responses in Arabidopsis. Mol Plant-Microbe Interact. 2020:33(3): 474–487. https://doi.org/10.1094/MPMI-09-19-0262-R
- **Granado J, Felix G, Boller T**. Perception of fungal sterols in plants (subnanomolar concentrations of ergosterol elicit extracellular alkalinization in tomato cells). Plant Physiol. 1995:**107**(2): 485–490. https://doi.org/10.1104/pp.107.2.485
- **Hauck P, Thilmony R, He SY**. A *Pseudomonas syringae* type III effector suppresses cell wall-based extracellular defense in susceptible Arabidopsis plants. Proc Natl Acad Sci USA. 2003:**100**(14): 8577–8582. https://doi.org/10.1073/pnas.1431173100
- Hirner A, Ladwig F, Stransky H, Okumoto S, Keinath M, Harms A, Frommer WB, Koch W. Arabidopsis LHT1 is a high-affinity transporter for cellular amino acid uptake in both root epidermis and leaf mesophyll. Plant Cell. 2006:18(8): 1931–1946. https://doi.org/10.1105/tpc.106.041012
- Huynh T, Dahlbeck D, Staskawicz B. Bacterial blight of soybean: regulation of a pathogen gene determining host cultivar specificity. Science. 1989:245(4924): 1374–1377. https://doi.org/10.1126/science.2781284
- Jeworutzki E, Roelfsema MRG, Anschütz U, Krol E, Elzenga JTM, Felix G, Boller T, Hedrich R, Becker D. Early signaling through the Arabidopsis pattern recognition receptors FLS2 and EFR involves Ca²⁺-associated opening of plasma membrane anion channels. Plant J. 2010:62(3): 367–378. https://doi.org/10.1111/j.1365-313X. 2010.04155.x
- Kunze G, Zipfel C, Robatzek S, Niehaus K, Boller T, Felix G. The N terminus of bacterial elongation factor tu elicits innate immunity in Arabidopsis plants. Plant Cell. 2004:16(12): 3496–3507. https://doi.org/10.1105/tpc.104.026765
- Lecourieux D, Lamotte O, Bourque S, Wendehenne D, Mazars C, Ranjeva R, Pugin A. Proteinaceous and oligosaccharidic elicitors induce different calcium signatures in the nucleus of tobacco cells. Cell Calcium. 2005:38(6): 527–538. https://doi.org/10.1016/j.ceca.2005.06.036
- **Liu G, Ji Y, Bhuiyan NH, Pilot G, Selvaraj G, Zou J, Wei Y**. Amino acid homeostasis modulates salicylic acid—associated redox status and defense responses in Arabidopsis. Plant Cell. 2010:**22**(11): 3845–3863. https://doi.org/10.1105/tpc.110.079392
- Lohaus G, Pennewiss K, Sattelmacher B, Hussmann M, Hermann Muehling K. Is the infiltration-centrifugation technique appropriate for the isolation of apoplastic fluid? A critical evaluation with

- different plant species. Physiol Plant. 2001:111(4): 457-465. https:// doi.org/10.1034/j.1399-3054.2001.1110405.x
- Lovelace AH, Smith A, Kvitko BH. Pattern-Triggered immunity alters the transcriptional regulation of virulence-associated genes and induces the sulfur starvation response in Pseudomonas syringae pv. Tomato DC3000. Mol Plant-Microbe Interact. 2018:31(7): 750-765. https://doi.org/10.1094/MPMI-01-18-0008-R
- Maintz J, Cavdar M, Tamborski J, Kwaaitaal M, Huisman R, Meesters C, Kombrink E, Panstruga R. Comparative analysis of MAMP-induced calcium influx in Arabidopsis seedlings and protoplasts. Plant Cell Physiol. 2014:55(10): 1813-1825. https://doi.org/ 10.1093/pcp/pcu112
- Nemkov T, D'Alessandro A, Hansen KC. Three-minute method for amino acid analysis by UHPLC and high-resolution quadrupole orbitrap mass spectrometry. Amino Acids. 2015:47(11): 2345-2357. https://doi.org/10.1007/s00726-015-2019-9
- Nicaise V, Roux M, Zipfel C. Recent advances in PAMP-triggered immunity against bacteria: pattern recognition receptors watch over and raise the alarm. Plant Physiol. 2009:150(4): 1638-1647. https:// doi.org/10.1104/pp.109.139709
- Nobori T, Velásquez AC, Wu J, Kvitko BH, Kremer JM, Wang Y, He SY, Tsuda K. Transcriptome landscape of a bacterial pathogen under plant immunity. Proc Natl Acad Sci USA. 2018:115(13): E3055-E3064. https://doi.org/10.1073/pnas.1800529115
- O'Leary BM, Neale HC, Geilfus C-M, Jackson RW, Arnold DL, Preston GM. Early changes in apoplast composition associated with defence and disease in interactions between Phaseolus vulgaris and the halo blight pathogen Pseudomonas syringae Pv. Phaseolicola. Plant Cell Environ, 2016:**39**(10): 2172–2184. https://doi.org/10.1111/pce.12770
- Park DH, Mirabella R, Bronstein PA, Preston GM, Haring MA, Lim CK, Collmer A, Schuurink RC. Mutations in y-aminobutyric acid (GABA) transaminase genes in plants or Pseudomonas syringae reduce bacterial virulence. Plant J. 2010:64(2): 318-330. https://doi. org/10.1111/j.1365-313X.2010.04327.x
- Pilot G, Stransky H, Bushey DF, Pratelli R, Ludewig U, Wingate VPM, Frommer WB. Overexpression of GLUTAMINE DUMPER1 leads to hypersecretion of glutamine from hydathodes of Arabidopsis leaves[W]. Plant Cell. 2004:16(7): 1827-1840. https://doi.org/10. 1105/tpc.021642
- Pratelli RR, Voll LM, Horst RJ, Frommer WB, Pilot G. Stimulation of nonselective amino acid export by glutamine dumper proteins. Plant Physiol. 2010:**152**(2): 762–773. https://doi.org/10.1104/pp.109. 151746
- Preston GM. Profiling the extended phenotype of plant pathogens: challenges in bacterial molecular plant pathology. Mol Plant Pathol. 2017:18(3): 443-456. https://doi.org/10.1111/mpp.12530
- Rahme LG, Mindrinos MN, Panopoulos NJ. Plant and environmental sensory signals control the expression of hrp genes in *Pseudomonas* syringae pv. Phaseolicola. J Bacteriol. 1992:174(11): 3499-3507. https://doi.org/10.1128/jb.174.11.3499-3507.1992
- Rico A, Preston GM. Pseudomonas syringae pv. Tomato DC3000 uses constitutive and apoplast-induced nutrient assimilation pathways to catabolize nutrients that are abundant in the tomato apoplast. Mol Plant-Microbe Interact. 2008:21(2): 269-282. https://doi.org/ 10.1094/MPMI-21-2-0269
- Smith A, Lovelace AH, Kvitko BH. Validation of RT-qPCR approaches to monitor Pseudomonas syringae gene expression during infection and exposure to pattern-triggered immunity. Mol Plant-Microbe

- Interact. 2018:31(4): 410-419. https://doi.org/10.1094/MPMI-11-17-0270-TA
- **Solomon PS, Oliver RP**. Evidence that γ -aminobutyric acid is a major nitrogen source during Cladosporium fulvum infection of tomato. Planta. 2002:**214**(3): 414–420. https://doi.org/10.1007/s00425010
- Solomon PS, Oliver RP. The nitrogen content of the tomato leaf apoplast increases during infection by Cladosporium fulvum. Planta. 2001:**213**(2): 241–249. https://doi.org/10.1007/s004250000500
- Toyota M, Spencer D, Sawai-Toyota S, Jiaqi W, Zhang T, Koo AJ, Howe GA, Gilroy S. Glutamate triggers long-distance, calcium-based plant defense signaling. Science. 2018:361(6407): 1112-1115. https:// doi.org/10.1126/science.aat7744
- Traxler MF, Summers SM, Nguyen H-T, Zacharia VM, Hightower GA, Smith JT, Conway T. The global, ppGpp-mediated stringent response to amino acid starvation in Escherichia coli. Mol Microbiol. 2008:68(5): 1128-1148. https://doi.org/10.1111/j.1365-2958.2008. 06229.x
- Tsuda K, Sato M, Glazebrook J, Cohen JD, Katagiri F. Interplay between MAMP-triggered and SA-mediated defense responses. Plant J. 2008:**53**(5): 763–775. https://doi.org/10.1111/j.1365-313X.2007. 03369 x
- Ward JL, Forcat S, Beckmann M, Bennett M, Miller SJ, Baker JM, Hawkins ND, Vermeer CP, Lu C, Lin W, et al. The metabolic transition during disease following infection of Arabidopsis thaliana by Pseudomonas syringae pv. Tomato. Plant J. 2010:63(3): 443-457. https://doi.org/10.1111/j.1365-313X.2010.04254.x
- Wildermuth MC, Dewdney J, Wu G, Ausubel FM. Isochorismate synthase is required to synthesize salicylic acid for plant defence. Nature. 2001:414(6863): 562-565. https://doi.org/10.1038/35107108
- Xin X-F, He SY. Pseudomonas syringae pv. Tomato DC3000: a model pathogen for probing disease susceptibility and hormone signaling in plants. Annu Rev Phytopathol. 2013:51(1): 473-498. https://doi. org/10.1146/annurev-phyto-082712-102321
- Xin X-F, Kvitko B, He SY. Pseudomonas syringae: what it takes to be a pathogen. Nat Rev Microbiol. 2018:16(5): 316-328. https://doi.org/ 10.1038/nrmicro.2018.17
- Yamada K, Saijo Y, Nakagami H, Takano Y. Regulation of sugar transporter activity for antibacterial defense in Arabidopsis. Science. 2016: 354(6318): 1427-1430. https://doi.org/10.1126/science.aah5692
- Yang H, Postel S, Kemmerling B, Ludewig U. Altered growth and improved resistance of Arabidopsis against Pseudomonas syringae by overexpression of the basic amino acid transporter AtCAT1. Plant Cell Environ. 2014:37(6): 1404-1414. https://doi.org/10.1111/pce. 12244
- Yu X, Lund SP, Scott RA, Greenwald JW, Records AH, Nettleton D, Lindow SE, Gross DC, Beattie GA. Transcriptional responses of Pseudomonas syringae to growth in epiphytic versus apoplastic leaf sites. Proc Natl Acad Sci USA. 2013:110(5): E425-E434. https://doi. org/10.1073/pnas.1221892110
- Zhang W, He SY, Assmann SM. The plant innate immunity response in stomatal guard cells invokes G-protein-dependent ion channel regulation. Plant J. 2008:56(6): 984-996. https://doi.org/10.1111/j.1365-313X.2008.03657.x
- Zhang X, Khadka P, Puchalski P, Leehan JD, Rossi FR, Okumoto S, Pilot G, Danna CH. MAMP-elicited changes in amino acid transport activity contribute to restricting bacterial growth. Plant Physiol. 2022:**189**(4): 2315–2331. https://doi.org/10.1093/plphys/kiac217